New Pyrazine Derivatives as Efficient Inhibitors on Mild Steel Corrosion in Hydrochloric Medium

Shuo Zhang*, Hongjun Li, Lin Wang, Dezheng Liu, Enshun Ping, Peng Zou, Tianli Ma, Nan Li

CNPC Bohai Drilling Engineering Company Limited, Tianjin, 300450, China.
sanl2016@163.com

Novel pyrazine derivatives PD-1 were synthesized and their inhibitive action against the corrosion of mild steel in 15% HCl solution was studied by weight loss, potentiodynamic polarization and electrochemical impedance spectroscopy (EIS) studies. Polarization studies showed that the studied inhibitors were of mixed type in nature. Scanning Electron Microscope (SEM) and Energy dispersive X-ray spectroscopy (EDX) were performed for surface study of uninhibited and inhibited mild steel samples. The pyrazine derivatives are arranged as mixed-type inhibitors in HCl. Inhibition efficiencies increased with increasing concentration of inhibitor. Data obtained from weight loss and electrochemical measurements have shown that the compound has the excellent inhibiting properties for mild steel in HCl solution. The results showed that pyrazine derivatives acted as an excellent and a mixed-type inhibitor via strongly chemical adsorption onto mild steel surface to suppress simultaneously both anodic and cathodic processes.

1. Introduction

The use of corrosion inhibitor is one of the most effective measures for protecting metal surfaces against corrosion in acid environments (Goulart et al., 2013; Edgar M and Edgar V, 2016; Xi 2016). Some organic compounds are found to be effective corrosion inhibitors for many metals and alloys. Generally, inhibitor molecules may physically or chemically adsorb on a corroding metal surface (Hassan et al., 2015).

In any case, adsorption is generally over the metal surface forming an adsorption layer that functions as a barrier protecting the metal from the corrosion (Ferdows et al., 2009). It has been commonly recognized that an organic inhibitor usually promotes formation of a chelate on a metal surface, by transferring electrons from the organic compounds to the metal and forming a coordinate covalent bond during the chemical adsorption. In this way, the metal acts as an electrophile; and the nucleophile centers of inhibitor molecule are normally heteroatoms with free electron pairs that are readily available for sharing, to form a bond. The power of the inhibition depends on the molecular structure of the inhibitor (Sciubba and Enrico, 2004). Organic compounds, containing functional electronegative groups and p-electron in triple or conjugated double bonds, are usually good inhibitors (Tourabi et al., 2013). Heteroatoms, such as sulfur, phosphorus, nitrogen and oxygen, together with aromatic rings in their structure are the major adsorption centers (Hegazy et al., 2013). The planarity (g) and the lonely electron pairs in the heteroatoms are important features that determine the adsorption of these molecules on the metallic surface (Becke, 1988).

Corrosion inhibitor is often added to mitigate the corrosion of metal by acid attack. Most well-known corrosion inhibitors are organic compounds containing polar groups including nitrogen, sulfur, and/or oxygen atoms and heterocyclic compounds with polar functional groups and conjugated double bonds (Li et al., 2009). The pyrazine derivatives are of great interest in organic chemistry (Bentiss et al., 2005), because manifold implications viz, antibacterial, antifungal, anticancer, antitumor, antiherpes, antiallergic, analgesic, antiinflammatory, and antineuplastic are well proved by a large number of publication on it (Cano et al., 2004). The selection of pyrazine derivatives as corrosion inhibitors is based on the presence of two nitrogen atoms in their structure, which facilitates electrophilic attack. Pyrazine derivatives are a very important class of nitrogen-containing compounds; it has pyrazine cycle annulated with the benzene ring (Tian et al., 2013). The pyrazine ring is a part of many polycyclic compounds of biological and/or industrial significance. Examples are

pyrazines, phenazines and bioluminescent natural products pteridines, flavins and their derivatives (Solmaz et al., 2008). All these compounds are characterized by a low-lying unoccupied π-molecular orbital and by the ability to act as bridging ligand. Due to these two properties pyrazine possess a characteristic reactivity(Oguzie et al., 2004). Pyrazines have been intensively investigated as effective corrosion inhibitors in different acid medium (Sudheer and Quraishi, 2013). Pyrazines and its different substituted derivatives e.g. (Ghailane et al., 2013)., bromo, methyl andamino, have different inhibition efficiency depending on the availability of lone pair of electrons on hetero atoms and also based on metal-heteroatom interactions of concerned metal in acid solutions (Klamt and Schüürmann., 1993).

2. Experimental

2.1 Mild steel sample
Corrosion studies were performed on N80 steel samples having composition (wt.%): C, 0.31; Mn, 0.92; Si, 0.19; S, 0.008; P, 0.010; Cr, 0.20 and Fe balance. N80 steel coupons were cut into the dimension 1.0 cm × 3.0 cm × 0.1 cm for weight loss experiments. For electrochemical measurements, N80 steel coupons having the dimension 1.0 cm× 1.0 cm × 0.1 cm were mechanically abraded and covered with araldite resin leaving an exposed surface area of 1 cm^2. Prior to the experiments, specimens were washed with distilled water, degreased in acetone, dried and stored in vacuum desiccator.

2.2 Test solution
Analytical reagent grade HCl was diluted with double distilled water to obtain 15% HCl solution. The concentration of inhibitors employed was varied from 10 × 10^{-5} to 1000 × 10^{-5} M, and the volume of the electrolyte used was 250 mL for weight loss measurements and 150 mL for electrochemical studies.

2.3 Synthesis of the inhibitor
A solution of o-phenylenediamine/ethylenediamine (1 mmol) and furil (1 mmol) in ethanol:water (7:3, 10 ml) was stirred at room temperature in the presence of catalytic amount of phenol (20 mol%, 0.01 g). The progress of the reaction was monitored by TLC (n-hexane-ethyl acetate 20:1). After completion of the reaction, water 20 ml) was added to the mixture and was allowed to stand at room temperature for 30 min. During this time, crystals of the pure product were formed which were collected by filtration and dried. For further purification, the products were recrystallized from hot ethanol and then PD-1 was got.

2.4 Weight loss method
Weight loss measurements were performed at the temperature 80℃. The accurately weighed mild steel test coupons were immersed for 6 h in 250 mL of 15% HCl solution in the absence and presence of different concentrations of the inhibitors (Xu et al., 2013).

The test coupons were then removed from the 15% HCl solution, washed thoroughly with distilled water, dried and weighed. Triplicate experiments were conducted for each concentration and temperature of the inhibitor for the reproducibility and the average of weight losses were taken to calculate different corrosion parameters. The corrosion rate (CR), inhibition efficiency (η%) and surface coverage (θ) were determined by the following equations (Khamis et al., 2013):

$$CR(mmy^{-1}) = \frac{8.76 \times 10^4 \times W}{D \times A \times t}$$

(1)

where, W=weight loss (g), A=area of specimen (cm^2) exposed in solution, t=exposure time (h), and D=density of mild steel (g cm^{-3}).

2.5 Potentiodynamic polarization studies
Potentiodynamic polarization measurements were carried out in a conventional three-electrode cell consisting of N80 steel working electrode, a platinum counter electrode and a saturated calomel electrode (SCE) as reference electrode. The CH electrochemical workstation (Model No: CHI 760D, manufactured by CH Instruments, Austin, USA) was used and the measurements were taken at 80℃. Before each measurement, the working electrodes were immersed in the test solution until a steady potential was reached. After the establishment of a steady open circuit potential (OCP), potentiodynamic polarization curves were obtained at a scan rate of 0.1 mV s^{-1} in the potential range from −700 to −300 mV vs SCE. Potentiodynamic polarization studies were performed in 15% HCl solution in the absence and presence of various concentrations of the three inhibitors. Corrosion current density (i$_{corr}$) and corrosion potential (E$_{corr}$) values were obtained by Tafel extrapolation method. The percentage inhibition efficiency (η%), was calculated using the equation:

$$\eta(\%) = \frac{i^0_{corr} - i_{corr}}{i^0_{corr}} \times 100 \tag{2}$$

where i^0_{corr} and i_{corr} are the values of corrosion current density without and with inhibitors, respectively.

2.6 Electrochemical impedance spectroscopy (EIS) studies

Impedance measurements were carried out using the same electrochemical cell and workstation as mentioned for polarization measurements in the frequency range from 100 kHz to 10 mHz, using 10 mV peak to peak amplitude ac signal at the OCP. The impedance spectra were recorded as Nyquist and Bode plots. The charge transfer resistance (R_{ct}) was obtained by fitting the impedance spectra with an appropriate equivalent circuit. The inhibition efficiency (η%) was calculated from the R_{ct} values according to the equation:

$$\eta(\%) = \frac{R_{ct(inh)} - R_{ct}}{R_{ct(inh)}} \times 100 \tag{3}$$

Where, $R_{ct(inh)}$ and R_{ct} are charge transfer resistances in with and without inhibitor respectively. The values of double layer capacitance (C_{dl}) were calculated from the R_{ct} and CPE parameters (Y_0 and n) using the expression (Lashkari and Arshadi , 2004)

$$C_{dl} = (Y_0 R_{ct}^{1-n})^{1/n} \tag{4}$$

Where, Y_0 is CPE constant and n is CPE exponent. The value of n represents the deviation from the ideal behavior and it lies between 0 and 1.

2.7 Scanning electron microscopic and energy dispersive spectroscopy analysis

The N80 steel specimens of size 1.0 cm× 1.0 cm× 0.1 cm were abraded with a series of emery paper (grade 320-500-800-1200) and then washed with distilled water and acetone (Pournazari et al, 2013). After immersion in 15% HCl solution in the absence and presence of 500 mg/l concentration of PD-1 at 80 ℃ for 6 h, the specimens were cleaned with distilled water, dried with a cold air blaster, and then the SEM and EDX images were recorded using the instrument HITACHI S3400N.

3. Results and discussion

3.1 Weight loss measurements

The variation of inhibition efficiency with different concentrations in 800 mg/l HCl at 80 ℃ is shown in Figure. 1. As can be seen from Figure. 1, with increasing concentration of inhibitors, the inhibition efficiency increased. It was observed that when the concentration reaches 1000 mg/l it gives 89.9% efficiency.
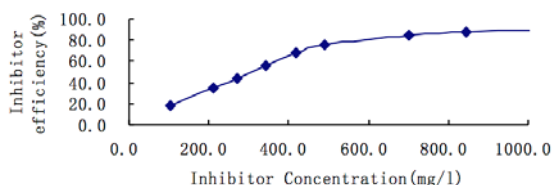
Figure 1: Variation of inhibition efficiency with different concentrations at 80℃.

3.2 Electrochemical impedance spectroscopic technique

Table 1: AC-impedance parameters for corrosion of mild steel in HCl

NO.	Con (mM)	Rct (Ohm cm^2)	Cdl (µF cm^{-2})	Inhibition efficiency (%)
1	0	15.26	38.1	-
2	0.5	82.91	25.4	80.56
3	5	109.5	23.1	86.21
NO.	Con (mM)	Rct (Ohm cm^2)	Cdl (µF cm^{-2})	Inhibition efficiency (%)

Electrochemical impedance spectroscopy (EIS) is an excellent technique that has been used in understanding the mechanism of corrosion and passivation phenomena of metals and alloys in their surrounding environments. EIS experiments were performed to report the effect of pyrazine and pyrazine derivatives on the inhibition of mild steel and to determine the kinetic parameters for electron transfer reactions at the mild steel/electrolyte interface (Issa et al., 2008).

The impedance results obtained in the presence and absence of inhibitors are presented as Nyquist plots in Figure 2. It is evident from the figure that MS exhibited typical impedance behavior in 15% HCl medium for all the inhibitors screened and displayed marked changes in impedance response for each concentration studied. This can be attributed to charge transfer of the corrosion process, the diameter of the semicircle increases with increasing inhibitor concentration. The semicircles in the impedance diagram indicate that the corrosion process is mainly controlled by the charge-transfer process. The main impedance parameters obtained are listed in Table 1. As can be seen from the Table 1, with increasing concentration of inhibitors, the measured values of charge-transfer resistance (R_{ct}) increased and the values of the double-layer capacitance (C_{dl}) decreased. The increase in the values of R_{ct} and inhibition efficiency are due to the formation of a protective surface film on the metal surface caused by the gradual replacement of water molecules by adsorbed inhibitor molecules. This results in an increase in the thickness of the electronic double layer, and a decrease in electrical capacitance. The decrease in C_{dl} occurred as a result of the decrease in the local dielectric constant, which suggests that the inhibitor molecules function by adsorption. The inhibition efficiencies obtained from different testing methods used in this study are comparable and in fair agreement.
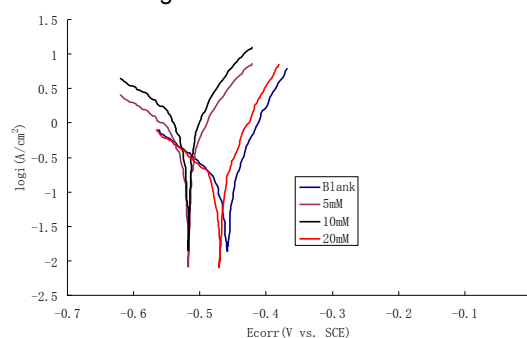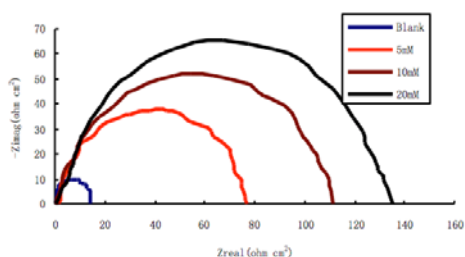
Figure 2: Nyquist plots for mild steel in 15% HCl solution containing various PD-1 concentrations at 80°C.

Figure 3: Potentiodynamic polarization curves for mild steel at 80°C.

Table 2: Electrochemical parameter and percentage inhibition efficiency in 15% HCl solution at 80°C

NO.	Conc. (ppm)	-Ecorr (mV/SCE)	Icorr ($\mu A\ cm^{-2}$)	βa (mV dec^{-1})	βc (mV dec^{-1})	θ	η(%)
1	0	422	6812	371	339	-	-
2	50	431	915	353	318	0.92	91.8
3	100	429	843	327	307	0.91	90.3
4	200	445	572	318	283	0.89	88.5
5	300	453	383	291	271	0.89	87.9
6	400	461	294	276	253	0.88	87.1

3.3 Potentiodynamic polarization technique

In order to know the kinetics of anodic and cathodic reactions, polarization experiments were carried out potentiodynamically in unstirred 15% HCl solution in the absence and presence of different concentration of inhibitors and the obtained polarization curves are shown in Figure 3. The corrosion kinetic parameters derived from these curves are presented in Table 2.

In acidic solutions, the anodic reaction is the movement of metal ions from the working electrode into the solution, and the cathodic reaction is the discharge of hydrogen ions to hydrogen gas or reducing the concentration of oxygen. The inhibitor may affect either the anodic or the cathodic reaction or both. Since the anodic Tafel slope and cathodic Tafel slope of pyrazines and pyrazines were found to change with inhibitor concentration, the inhibitors affected both these reactions and acted as mixed-type inhibitors. A close examination of Figure 3 reveals that the addition of inhibitors to 15% HCL affects both the anodic and cathodic parts of the curve. Theoretically, no shifts in E_{corr} should be observed after addition of the corrosion inhibitors if the geometric blocking effect is stronger than the energy effect. The change observed in the E_{corr} values upon addition of the inhibitors therefore indicates that the energy effect is stronger than the blocking effect. It can be

seen from the table 2 that the corrosion current density I_{corr} decreased noticeably with increase in inhibitor concentration and the corrosion potential E_{corr} of mild steel shifts toward less negative direction, which suggests that the inhibitors behave as very good corrosion inhibitors for mild steel in 1 M HCl solution. The anodic Tafel curves in the acidic solution containing the inhibitor is shifted to the direction of the lower current density, which suggests that the inhibitor could also suppress the anodic reaction. An inhibitor can be classified as an anodic or cathodic type when the change in E_{corr} value is larger than 85 mV. However, in the present study, the largest displacement exhibited by the inhibitors was less than 85 mV, from which it can be concluded that all the inhibitors act as mixed type inhibitors.

3.4 SEM and EDS studies

(a)   (b)
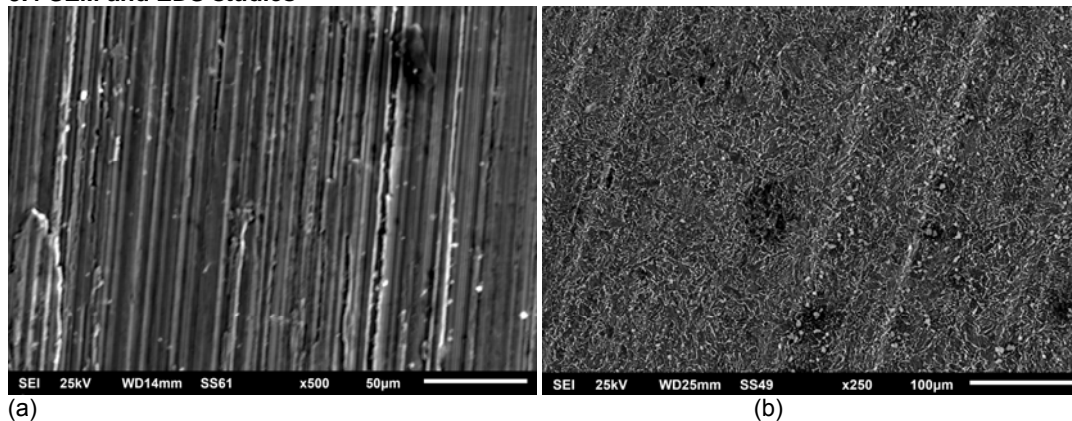
Figure 4: SEM image of mild steel (a) before immersion, (b) after immersion with inhibitor.

Table 3: Percentage atomic contents of elements obtained from EDX spectra

Sample	Fe	C	Cr	Mn	Cl	N	O
Mild steel	85.29	12.39	0.87	0.49	-	-	-
Mild steel in HCl	83.75	15.99	0.69	0.29	2.31	-	6.31
Mild steel in Inhibitor	69.73	17.39	0.67		0.33	3.67	8.55

SEM photomicrographs for mild steel in 15% HCl solution in the absence and presence of 200 ppm of PD-1 are shown in Figure 4. The surface of the polished mild steel specimen (Figure. 4a) is very smooth and shows no corrosion while mild steel specimen dipped in 15%HCl solution in the absence of inhibitor (Figure. 4b) is very rough and the surface is damaged due to metal dissolution. The EDS analysis of the specimen in the absence of the inhibitor indicates the presence of Fe and O, which shows that the passive film on the mild steel surface contained only Fe_2O_3.
A comparable elemental distribution is shown in Table 3. The obtained atomic weight% values of the elements from the EDS spectra of inhibited mild steel surface show more intensity of nitrogen and carbon which are present in PD-1. The values of atomic weight% of Fe in the inhibited acid is less compared to blank. This confirms the presence of inhibitor on the mild steel surface.

4. Conclusions

This study has revealed that the inhibition efficiencies of the studied compound PD-1 tended to increase with increasing inhibitor concentration. Polarization measurements show that they are mixed-type inhibitors. The corrosion inhibition was studied in HCl for mild steel using weight loss and electrochemical techniques. It was observed that the inhibition efficiency of PD-1 acid increases with increase in the inhibitor concentration. The inhibitor showed maximum inhibition efficiency of 89.9% at 1000 mg/l inhibitor concentration. Impedance studies showed that PD-1 acid inhibits through adsorption mechanism. It was further supported by surface morphology studies using SEM and EDX techniques. PD-1 acid is proved as an efficient inhibitor having mixed type of inhibitor properties. The adsorption of the studied inhibitors on mild steel followed the Langmuir adsorption.

Reference

Becke A.D., 1988, A multicenter numerical integration scheme for polyatomic molecules, J. Chem. Phys. 88, 2547–2553.

Bentiss F., Lebrini M., Lagrenée M., 2005, Thermodynamic characterization of metal dissolution and inhibitor adsorption processes in mild steel/2, 5-bis(n-thienyl)-1, 3, 4-thiadiazoles/hydrochloric acid system, Corros. Sci. 47, 2915-2931.

Cano E., Polo J.L., Bastidas J.M., 2004, A study on the adsorption of benzotriazole on copper in hydrochloric acid using the inflection point of the isotherm, Adsorption. 10, 219-225.

Edgar M., Edgar V., 2016, State evaluation of steel bridges of the Colombian National roadway network, Revista de la Facultad de Ingeniería, 31(5), 462-489

Ferdows, M., Crepeau, J.C., Postelnicu A., 2009, Natural convection flow with wall temperature considering internal heat generation, International Journal of Heat and Technology, 27(1), 109-112.

Ghailane T., Balkhmima R.A., Ghailane R., 2013, Experimental and theoretical studies for mild steel corrosion inhibition in 1 M HCl by two new benzothiazine derivatives, Corros. Sci. 76, 317-324.

Goulart C.M., Esteves-Souza A., Martinez-Huitle C.A., 2013, Experimental and theoretical evaluation of semicarbozones and thiosemicarbazones as organic corrosion inhibitors, Corros. Sci. 67, 281-291.

Hassan, Anthony R., Gbadeyan, Jacob A., 2015, A reactive hydromagnetic internal heat generating fluid flow through a channel, International Journal of Heat and Technology, 33, 43-50. DOI: 10.18280/ijht.330306.

Hegazy M.A., Badawi A.M., Kamel W.M., 2013, Corrosion inhibition of carbon steel using novel N-(2-(2-mercapto acetoxy)ethyl)-N, N-dimethyl) dodecan-1-aminium bromide during acid pickling, Corros. Sci. 69, 110-122.

Hu S.Q., Hu J.Q., Fan C.C., 2010, Theoretical and experimental study of corrosion inhibition performance of new imidazoline corrosion inhibitors, Acta Chim. Sinica, 68, 2051-2058.

Issa R.M., Awad M.K., Atlam F.M., 2008, Quantum chemical studies on the inhibition of corrosion of copper surface by substituted uracils, Appl. Surf. Sci. 255, 2433-2441.

Khamis A., Saleh M.M., Awad M.I., 2013, El-Anadouti, Enhancing the inhibition action of cationic surfactant with sodium halides for mild steel in 0.5 M H_2SO_4, Corros. Sci. 74, 83-91.

Klamt A., Schüürmann G., 1993, A new approach to dielectric screening in solvents with explicit expressions for the screening energy and its gradient, J.Chem. Soc. Perkin. Trans. 2, 799-805.

Lashkari M., Arshadi M.R., 2004, DFT studies of pyridine corrosion inhibitors in electrical double layer: solvent, substrate, and electric field effects, Chem. Phys. 299, 131-137.

Lee C., Yang W., Parr R.G., 1988, Development of the Colle-Salvetti correlation-energy formula into a functional of the electron density, Phys. Rev. B. 37, 785-789.

Li W.H., He Q., Zhang S.T., 2008, Some new triazole derivatives as inhibitors for mild steel corrosion in acidic medium, J. Appl. Electrochem. 38, 289-295.

Li X.H., Deng S.D., Fu H., 2009, Inhibition effect of 6-benzylaminopurine on the corrosion of cold rolled steel in H2SO4 solution, Corros. Sci. 51, 620-634.

Oguzie E.E., Unaegbu C., Ogukwea C.N., 2004, Inhibition of mild steel corrosion in sulphuric acid using indigo dye and synergistic halide additives, Mater. Chem. Phys. 84, 363-368.

Pournazari Sh., Moayed M.H., Rahimizadeh M., 2013, In situ inhibitor synthesis from admixture of benzaldehyde and benzene-1, 2-diamine along with FeCl3 catalyst as a new corrosion inhibitor for mild steel in 0.5M sulphuric acid, Corros. Sci. 71, 20-31.

Sciubba, Enrico, 2004, Synthesis of heat exchanger networks performed by an expert design assistant based on second law reasoning, International Journal of Heat and Technology, 22(1), 37-49

Solmaz R., Kardas G., Yazici B., 2008, Adsorption and corrosion inhibitive properties of 2-amino-5-mercapto-1, 3, 4-thiadiazole on mild steel in hydrochloric acid media, Colloids Surf. A, 312, 7-17.

Sudheer, M.A. Quraishi, 2013, Electrochemical and theoretical investigation of triazole derivatives on corrosion inhibition behavior of copper in hydrochloric acid medium, Corros. Sci. 70, 161-169.

Tian H., Li W., Cao K., 2013, Potent inhibition of copper corrosion in neutral chloride media by novel thiadiazole derivatives, Corros. Sci. 73, 281–291.

Tourabi M., Nohair K., Traisnel M., 2013, Electrochemical and XPS studies of the corrosion inhibition of carbon steel in hydrochloric acid pickling solutions by 3, 5-bis(2-thienylmethyl)-4-amino-1, 2.4-triazole, Corros. Sci. 75, 123-33.

Xi G.Q., 2016, Design of an oil pipeline nondestructive examination system based on ultrasonic testing and magnetic flux leakage, Revista de la Facultad de Ingeniería, 31(5), 132-140

Xu B., Liu Y., Yin X.S., 2013, Experimental and theoretical study of corrosion inhibition of 3-pyridinecarbozalde thiosemicarbazone for mild steel in hydrochloric acid, Corros. Sci. 74, 206-213.